12188–12203 *Nucleic Acids Research, 2020, Vol. 48, No. 21* *Published online 9 November 2020*
doi: 10.1093/nar/gkaa974

Multiple biochemical properties of the p53 molecule contribute to activation of polymerase iota-dependent DNA damage tolerance

Stephanie Biber[1,*], Helmut Pospiech[2,3], Vanesa Gottifredi[4] and Lisa Wiesmüller[1,*]

[1]Department of Obstetrics and Gynecology, Ulm University, Ulm 89075, Germany, [2]Project group Biochemistry, Leibniz Institute on Aging – Fritz Lipmann Institute, D-07745 Jena, Germany, [3]Faculty of Biochemistry and Molecular Medicine, FIN-90014 University of Oulu, Finland and [4]Cell Cycle and Genomic Stability Laboratory, Fundación Instituto Leloir, Buenos Aires C1405BWE, Argentina

Received July 16, 2020; Revised October 05, 2020; Editorial Decision October 06, 2020; Accepted October 09, 2020

ABSTRACT

We have previously reported that p53 decelerates nascent DNA elongation in complex with the translesion synthesis (TLS) polymerase ι (POLι) which triggers a homology-directed DNA damage tolerance (DDT) pathway to bypass obstacles during DNA replication. Here, we demonstrate that this DDT pathway relies on multiple p53 activities, which can be disrupted by *TP53* mutations including those frequently found in cancer tissues. We show that the p53-mediated DDT pathway depends on its oligomerization domain (OD), while its regulatory C-terminus is not involved. Mutation of residues S315 and D48/D49, which abrogate p53 interactions with the DNA repair and replication proteins topoisomerase I and RPA, respectively, and residues L22/W23, which disrupt formation of p53-POLι complexes, all prevent this DDT pathway. Our results demonstrate that the p53-mediated DDT requires the formation of a DNA binding-proficient p53 tetramer, recruitment of such tetramer to RPA-coated forks and p53 complex formation with POLι. Importantly, our mutational analysis demonstrates that transcriptional transactivation is dispensable for the POLι-mediated DDT pathway, which we show protects against DNA replication damage from endogenous and exogenous sources.

INTRODUCTION

DNA damage tolerance (DDT) facilitates the progression of replication forks that have encountered obstacles on the template strand. Such bypass events are achieved either by the activation of translesion DNA synthesis (TLS) involving specialized polymerases or by homology-directed DDT via fork reversal or template-switch (1). A prerequisite for DDT is proliferation cell nuclear antigen (PCNA) ubiquitination (1). Thus, monoubiquitination triggers the switch from replicative to TLS polymerases, while polyubiquitination induces homology-directed DDT mechanisms (1). Recently, we discovered that p53 promotes slow-down of nascent DNA synthesis protecting from DNA replication-associated damage with a pro-survival outcome (2,3). Surprisingly, a deceleration of DNA replication relied on the formation of a complex of p53 and the TLS polymerase iota (POLι). This p53 function was lost in an exonuclease-deficient but transcriptionally active p53(115N) mutant. This supports a model implying idling events of iterative nucleotide incorporation and removal steps performed by the highly error-prone POLι and the intrinsic 3′-5′-exonuclease activity of p53. The p53–POLι idling complex was required to activate the helicase-like transcription factor (HLTF), an E3 ligase mediating PCNA polyubiquitination, and SWI/SNF catalytic subunit (SNF2) translocase zinc finger ran-binding domain containing 3 (ZRANB3), which catalyzes fork reversal to bypass the replication barrier via homology-directed DDT (3,4).

The p53 protein comprises a transcriptional transactivation domain (TAD, amino acids [aa] 1–42) at its N-terminus, followed by a proline-rich domain (PRD, aa 61–94), a central DNA binding domain (DBD, aa 102–292), an oligomerization domain (OD, aa 324–355) and a basic extreme C-terminal domain (BD, aa 364–393) (5). Most of the *TP53* missense mutations detected in tumor tissues are located within the DBD, particularly six hotspots including codons altering amino acids R248 and R273 which contact the DNA phosphate backbone (6). The N-terminus of p53, in particular the TAD, is necessary for its well-known function in transcriptional transactivation of genes and further serves as binding site for protein interaction partners unrelated to transcription, e.g. Replication Protein A (RPA), Polymerase beta (POLβ) and also to its nega-

*To whom correspondence should be addressed. Tel: +49 731 50058800; Fax: +49 731 500 58804; Email: lisa.wiesmueller@uni-ulm.de
Correspondence may also be addressed to Stephanie Biber. Tel: +49 731 500 58809; Fax: +49 731 500 58804; Email: stephanie.hampp@uni-ulm.de

tive regulator MDM2 (7–9). p53 requires the OD to adopt the active conformation for high affinity DNA binding as a protein tetramer (10,11). The C-terminal end of p53 is involved in a plethora of physical interactions, which impacts on its regulatory functions of the DBD. Thus, it binds DNA in a non-specific fashion, poly(ADP-ribose) as well as various proteins involved in transcription and DNA repair (12,13). In this study we addressed the specific role of distinct biochemical properties of the p53 molecule in the bypass of replication barriers in concert with POLι. To this end we investigate (i) replication-associated recombination as a measure of homology-directed DDT, (ii) the dynamics of nascent DNA synthesis and (iii) the interactions of relevant DDT pathway components after mutational loss-of-specific p53 activities. Our data demonstrate that the p53-POLι-dependent DDT pathway requires cooperative DNA binding by p53 tetramers as well as interactions of p53 with topoisomerase I, RPA and POLι at sites of replication barriers.

MATERIALS AND METHODS

Recombination measurements

K562 cells with chromosomally integrated recombination substrate, K562(HR-EGFP/3′EGFP) (14), were co-transfected with p53 expression plasmids or overexpression plasmids as detailed in Figure legends or in the Supplemental Information. Recombination frequencies were measured 72 h after transfection by quantification of 1 million cells from EGFP-positive cells within the life cell-population (SSC/FSC gate). For experiments with DNA cross-linker-treatment, cells were treated for 45 min with MMC (3 μM) directly after the electroporation, washed and re-incubated in fresh medium for additional 72 h.

Co-Immunoprecipitation and expression analysis

K562 cells were transfected with expression plasmid for p53(WT), p53(22Q/23S) or empty vector (ctrl). 48 h after transfection immunoprecipitation was performed. Cells were lysed in 50 mM Tris, pH 8; 150 mM NaCl; 1% NP40; complete protease inhibitor (Roche). The following antibodies were used for immunoprecipitation: polyclonal rabbit POLι-antibody (Bethyl, A301–304A) directed against POLι or as control: control—rabbit IgG fraction (Santa Cruz). Protein-extract and protein G Sepharose (PGS) were rotated over night at 4°C to remove components unspecifically binding to PGS. In parallel, antibody-PGS mixtures were rotated at 4°C. Afterwards, protein-extracts were separated from PGS by centrifugation and the supernatants transferred to the antibody–PGS mixtures, followed by rotation at 4°C for additional 4 h. After spin-down, precipitated proteins were washed five times with lysis buffer and dissolved in SDS-PAGE sample buffer. For Western blot analysis, protein extracts were separated electrophoretically, transferred to membranes and proteins were immunodetected via chemiluminescence. For immunostaining the antibodies were used as described in the Supplemental Materials and Methods. Chemiluminescence detection and quantification of protein levels were carried out in the linear range using ImageLab software on a ChemiDocMP System (BioRad). Values for the protein of interest were corrected with values of the loading control.

DNA fiber spreading assay

Cells were labeled with CldU (5-chloro-2-deoxyuridine, Sigma-Aldrich) for 20 min, washed twice with pre-warmed PBS before labeling cells with IdU (5-iodo-2-deoxyuridine, Sigma-Aldrich) in ten times higher concentration for another 20 min. During the IdU pulse, cells were either treated with MMC (3 μM) or H_2O as control. For TRC-experiments cells were pre-treated with DRB (20 μM) or its solvent DMSO 60 min prior to start of CldU-labeling and throughout the whole CldU- as well as IdU-labeling. Subsequently, cells were washed, harvested and resuspended in PBS. 2500 cells were transferred to a slide, lysed with 6 μl of 0.5% SDS, 200 mM Tris–HCl, pH7.4, 50 mM EDTA, and incubated at room temperature for 6 min. Slides were tilted about 20° to allow DNA to spread via gravity, covered with aluminum foil, air-dried for 7 min, fixed for 5 min with 3:1 methanol:acetic acid (prepared fresh), air dried for 7 min, and stored in 70% ethanol at 4°C overnight or directly afterwards processed for denaturation/deproteination in 2.5 N HCl for 1 h, followed by Immunofluorescence staining

Immunofluorescence staining

Saos-2 cells were grown on coverslips and fixed whereas K562 cells were spun onto cytospin glass slides and fixed with 3.7% formaldehyde in PBS at indicated time-points after MMC-treatment. Pre-extraction (1 min) was performed after Cytospin and before fixation of the cells (300 mM Sucrose, 50 mM NaCl, 20 mM HEPES (pH 7.4), 3 mM MgCl2, 1 mM EDTA, 0.5% (v/v) Triton X-100 in water). Permeabilization was performed with 0.5% Triton X-100 (Sigma-Aldrich) for 12 min at RT. Blocking unspecific binding sites was performed by use of 5% goat serum in PBS for 1 h. Immunostaining for 1 h at 37°C was performed with the primary antibodies listed in the Supplemental Materials and Methods and was followed by an incubation time of 45 min at 37°C with the secondary antibodies AlexaFluor555 (anti-rabbit/mouse, Invitrogen) or AlexaFluor488 (anti-mouse, Invitrogen). Immunofluorescence microscopy of nuclear signals was performed with Keyence BZ-9000 microscope (Keyence). Automated quantification of foci was carried out using BZ-II Analyser software. Intensity threshold and minimal focus size were maintained throughout one set of simultaneously treated and processed samples, both when detecting single green or red foci.

Immunofluorescence staining after DNA fiber spreading assays was performed by incubation with primary antibodies [1 h, room temperature (RT)]: anti-BrdU for detection of IdU (mouse, mAb, clone B44, BD BioScience #347580) and anti-BrdU for detection of CldU (rat, mAb, clone BU1/75 [ICR1] BioRad #OBT0030 or Novus #NB500-169 or Abcam #ab6326) after blocking with 5% BSA (45 min). As secondary antibodies, AlexaFluor555 (anti-mouse, Invitrogen) or AlexaFluor488 (anti-rat, Invitrogen) were used. DNA fibers were imaged with Keyence BZ-9000 microscope (Keyence, Neu-Isenburg, Germany). Measurements

of DNA fiber track lengths were carried out with BZ-II Analyser software or using FiJi (Fiji is just ImageJ) software [ImageJ Wiki, Laboratory for Optical and Computational Instrumentation, University of Wisconsin-Madison, Wisconsin, USA, (15)].

In situ proximity ligation assay (PLA)

K562 cells were transfected with the respective expression plasmids and spun onto poly-L-Lysine coated slides via cytospinning. H1299 cells were grown on chamber slides (Falcon® Culture Slides 4-well, OMNILAB, Bremen, Germany). Before fixing the cells with 3.7% formaldehyde in PBS (10 min), pre-extraction was performed for 1 min with pre-extraction buffer (300 mM Sucrose, 50 mM NaCl, 20 mM HEPES (pH 7.4), 3 mM MgCl2, 1 mM EDTA, 0.5% (v/v) Triton X-100 in water). The *in situ* proximity ligation assay (PLA) was carried out according to the manufacturer (Sigma-Aldrich). Blocking was performed using 5% goat serum in PBS for 1 h at RT or Duolink Blocking solution (Sigma-Aldrich) for 1 h at 37°C. Then cells were double-labeled for 1 h at 37°C using the primary antibodies as indicated in the Supplemental Material and Methods. PLA-stain was then performed using Duolink® PLA (Proximity Ligation assay to detect protein interaction) technology from Sigma-Aldrich. Therefore glass slides were stained with Duolink® In Situ PLA® Probe Anti-Rabbit PLUS (Affinity purified Donkey anti-Rabbit IgG (H+L), Sigma-Aldrich, DUO92002) and Duolink® In Situ PLA® Probe Anti-Mouse MINUS (Affinity purified Donkey anti-Mouse IgG (H+L), Sigma-Aldrich, DUO92004) for 1 h at 37°C. After washing the samples were then incubated with the Ligation-Ligase solution for 30 min at 37°C to hybridize oligonucleotides tagged on probes. After two short washing steps the glass slides were incubated with the Amplification-Polymerase solution for 100 min at 37°C to amplify hybridized oligonucleotides and fluorescently label the amplification products. Ligation and Amplification were performed with Duolink® In Situ Detection Reagents Orange (Sigma-Aldrich, DUO92007). Then, glass slides were covered with coverslips using Duolink® In Situ Mounting Medium with DAPI (Sigma-Aldrich, DUO82040). Imaging was performed using Keyence BZ-9000 microscope (Keyence). Automated quantification of PLA-foci was carried out with BZ-II Analyser software.

Plasmids

The following plasmids all encoding human p53 were previously described: pCMV-Wtp53 for expression of p53(WT) and pCMV-p53(315A) for expression of p53 with mutation S315A abrogating binding of p53 to topo-I (15), pCMV-p53(248W) and pCMV-p53(273H) for expression of the two hotspot p53 mutants with aa exchanges R248W and R273H (16), pCMV-p53(22Q/23S) for expression of p53 with the two aa exchanges L22Q and W23S (17). pCMV-p53(ΔN), pCMV-p53(ΔO) and pCMV-p53(ΔC) were kindly provided by Klaus Römer and are expression plasmids for expression of the p53 variants having lost aa 1–79, aa 327–342 and aa 370–393, respectively. pCMV-p53(48H/49H) were commercially cloned by Amsbio to mutate the ORF plasmid RC200003 for expression of human p53 (Myc-DDK tagged) with aa exchanges D48H (nucleotide sequence GAC to CAC) and D49H (nucleotide sequence GAT to CAT) which were previously described to disrupt RPA-binding (8). Plasmids for expression of human p21 and MDM2, namely pcDNA3-HA p21 were a gift from Jaewhan Song (Addgene plasmid #78782; http://n2t.ne/addgene:78782;RRID:Addgene_78782) and pcDNA3-MDM2 WT from Mien-Chie Hung (Addgene plasmid #16233; http://n2t.net/addgene:16233;RRID:Addgene_16233).

Transfection

Plasmids were transiently introduced in K562 and K562(HR-EGFP/3′EGFP) via electroporation (GenePulser Xcell, BioRad) as described in (3). In Saos-2 cells plasmids were transiently introduced using Amaxa reagents (Lonza, Cologne, Germany).

Statistics

Graphic presentation of data was performed using GraphPadPrism8.4 software (La Jolla, CA, USA). For calculation of statistically significant differences in recombination measurements Kruskal-Wallis test followed by Mann–Whitney two-tailed test was used. For calculation of statistically significant differences in DNA fiber spreading analysis and immunofluorescence experiments Kruskal-Wallis-test (Dunns-multiple comparison test) was used.

RESULTS

Replication-associated recombination by p53 depends on its DNA binding domain

We have previously shown that wild-type p53 (p53[WT]) but not the 3′-5′exonuclease deficient mutant p53(115N) triggers bypass of replication barriers which can be monitored via measurements of spontaneous replication-associated recombination (3). To determine the specific contribution of the DNA binding activities of p53 to such a resolution of replication barriers we monitored spontaneous, DSB-independent recombination frequencies of a chromosomally integrated *EGFP* substrate (Figure 1A) (14) in the p53-negative K562 leukemia cell model previously established by us (3,14,16). We compared the effect of p53(WT) to the one of cancer-related hotspot and sequence-specific DNA binding defective mutants p53(248W) and p53(273H), a mutant with a deleted oligomerization domain (p53ΔO, missing amino acids [aa] 327–346) and a mutant devoid of the non-sequence-specific DNA binding C-terminus (p53ΔC, missing aa 370–393) (Figure 1B). Expression of p53 was confirmed for all mutants and the p53 target p21 was upregulated only by p53(WT) and 53ΔC (Figure 1C). p53(WT) expression caused a robust increase (6- and 7-fold) of the recombination frequencies when compared to control samples (Figure 1B). In contrast, expression of p53(248W), p53(273H) and p53ΔO did not change the recombination frequencies when comparing them to control samples transfected with empty vector (Figure 1B). Expression of p53ΔC caused an increase of the recombination frequencies which was even higher than the one observed for

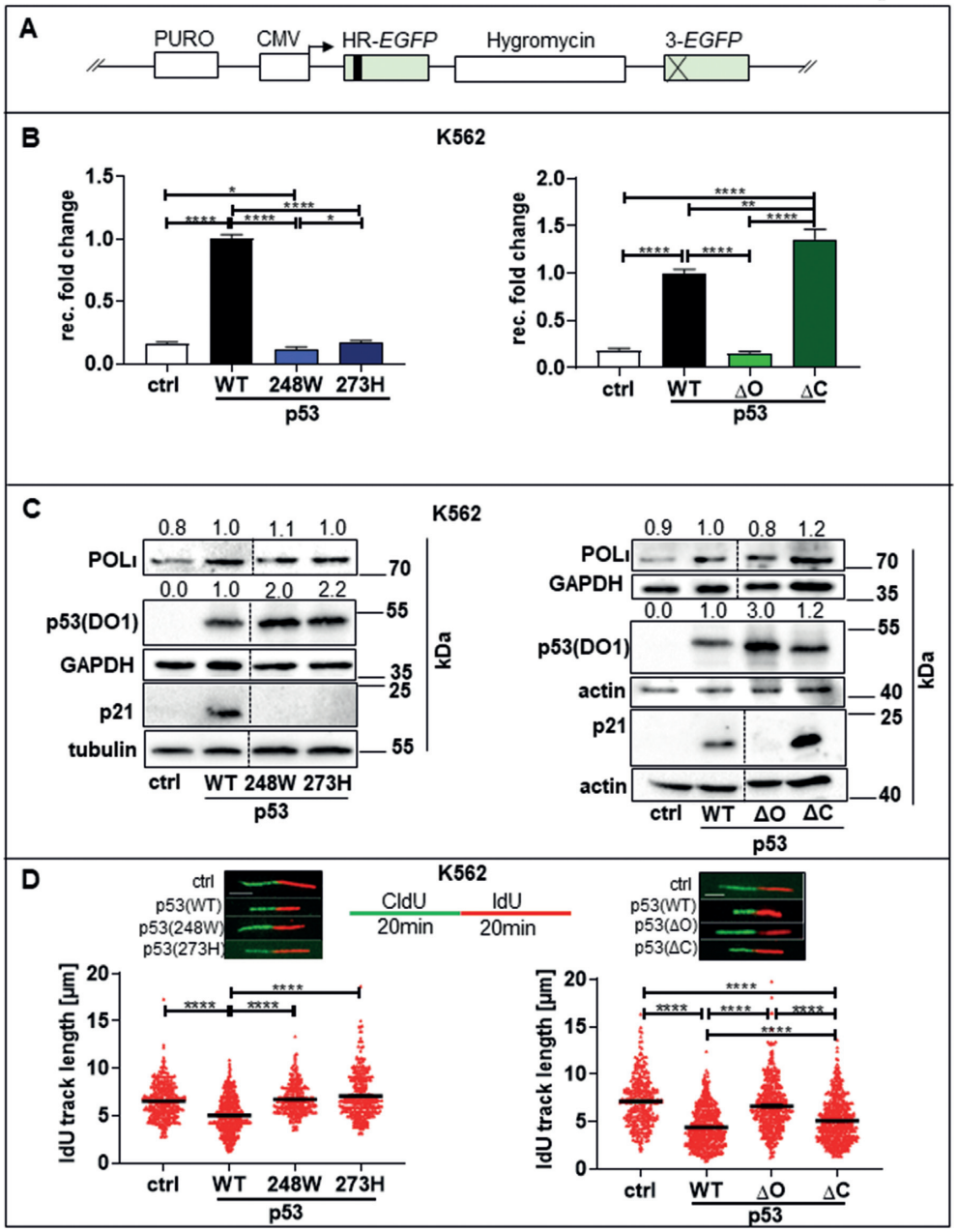

Figure 1. Analysis of the DNA binding defective p53 mutants p53(R248W), p53(R273H), p53ΔO and p53ΔC in replication-associated recombination and replication dynamics. K562(HR-EGFP/3′-EGFP) (**B**) or K562 parental (**C**, **D**) cells were transfected with expression plasmids for p53(WT), p53(248W), p53(273H), p53(ΔO), p53(ΔC) or empty vector (ctrl). 48 h (C, D) or 72 h (B) after transfection flow cytometry analysis (B), protein harvesting (C) or DNA fiber analysis (D) were performed. For graphic presentation, calculation of SEM and statistically significant differences via Kruskal-Wallis test followed by Mann–Whitney U test (B) or Dunns multiple comparison test (D) GraphPadPrism8.4 software was used. $*P < 0.05$, $**P < 0.01$, $***P < 0.001$, $****P < 0.0001$. (**A**) Schematic presentation of the EGFP-based recombination substrate (HR-EGFP/3′-EGFP). K562(HR-EGFP/3′-EGFP) cells with chromosomally integrated substrate were used to determine the recombination (rec.) fold changes (15). Hygromycin = hygromycin resistance cassette; PURO = puromycin resistance cassette. The kinked arrow indicates the promotor, the black square a frameshift mutation within the chromophore coding region resulting in an inactive HR-*EGFP* mutant, the cross replacement of the *EGFP* start codon by two stop codons generating an inactive 3′-EGFP mutant. (B) Role of p53′s DNA binding activity in recombination regulation. Recombination (rec.) fold changes were analyzed by flow cytometry via quantification of EGFP-positive cells. Measurements were individually corrected for transfection efficiencies. Mean values from p53(WT) expressing cells were set to 1 (absolute mean frequencies: 3×10^{-4} [left panel] and 3×10^{-5} [right panel]). Data were obtained from 12 individual measurements each. (C) p53 protein expression levels in K562 cells. Western blot analysis of the indicated p53 variants in whole cell lysates. Cell extract were harvested 48h after transient transfection. GAPDH (left panel) or Actin (right panel) served as loading controls. (D) Role of p53′s DNA binding activity in nascent DNA synthesis. Graphic overview in the upper panel shows the experimental outline and representative fibers. Both, CldU- and IdU-tracks were measured but for clarity graphic presentations focus on IdU-tracks in ongoing forks (emanating from a CldU-track). Lengths were obtained from ≥247 fibers (left panel) and ≥319 fibers (right panel) in two independent biological experiments each. Bars indicate SEM. Only statistically significant differences ≥0.0001 are shown (scale bar: 5 μm).

p53(WT) (Figure 1B). Similar results were observed when adding the DNA crosslinking agent Mitomycin C (MMC, 3 μM, 45 min) to cells expressing p53(WT) (5-fold increase), and p53(248W) or p53(273H) (no increase) (Supplementary Figure S1A). MMC-treatments were included as controls for our microscopic studies later on, where it raises the sensitivity for detection of transiently appearing protein complexes (3). It should be mentioned that MMC treatment did not trigger a statistically significant increase in the recombination events ($P = 0.4687$, Figure 1, Supplementary Figure S1A). This is anticipated since MMC damage within the *EGFP* reporter gene region is expected to occur extremely rare.

As reported previously by us, silencing of POLι decreased the recombination frequencies in the presence of p53(WT) (3). Importantly, POLι silencing had a similar effect in p53ΔC expressing cells, reducing the recombination frequency in a proportion that was similar to the one observed for p53(WT) (Supplementary Figure S1B). This result further supports the dependence on POLι of the homology-directed DDT function of p53 (3). Since our previous work revealed an association between p53 function in replication-associated recombination and in decelerating nascent DNA synthesis, we explored the effect of these p53 mutants on DNA replication speed using the DNA fiber spreading assay (3). Following sequential incorporation of 5-chloro-2-deoxyuridine (CldU) and 5-iodo-2-deoxyuridine (IdU), we observed shortening of DNA replication tracks in p53(WT) expressing K562 cells when comparing them with mock transfected samples. In contrast, the expression of neither p53(248W), p53(273H) nor p53ΔO caused changes in the DNA track lengths (Figure 1D). In line with its effect on recombination, track lengths of p53ΔC expressing K562 cells were shorter than in the p53-negative control albeit intermediate when also compared with the tracks of p53(WT) expressing K562 cells (Figure 1D). Similar results were obtained in MMC-treated K562 cells as well as MMC-treated Saos-2 cells, except that no significant difference was observed when comparing the IdU pulse track lengths of p53(WT) and p53ΔC (Supplementary Figure S1C, D). As expected, MMC-treatment shortened replication tracks, whereby p53(WT) further decreased the replication fork speed. Notably, data obtained in H1299 non-small cell lung carcinoma cell clones stably expressing inducible p53(WT) and p53(248W) showed replication phenotypes similar to the one obtained with K562 cells as well as Saos-2 cells transiently expressing these proteins (Supplementary Figure S1F) Taken together, our results suggest that the sequence-specific DNA binding activity of p53 tetramers is required for the p53-dependent regulation of replication fork progression under both conditions of unperturbed growth and of MMC-induced replication deceleration.

Replication-associated recombination by p53 depends on C-terminal and N-terminal interactions regardless of transcriptional activation

Having described the importance of p53′s DNA binding functions, we wanted to decipher the relevance of p53's interactions with DNA repair and replication proteins for their role in DDT. Topoisomerase-I (topo-I) releases torsional stress during DNA replication and transcription (18) and binds p53 between the core and OD via aa 302–321 following phosphorylation of S315 by Cyclin A1/CDK (19). The topo-I-binding defective mutant p53(315A) is impaired in recombination-stimulatory functions while it fully retains TA activities (16). In contrast to p53(WT), p53(315A) expressing cells revealed low recombination frequencies which were similar to those detected in p53-negative control samples (Figure 2A). Since both p53(WT) and p53(315A) were transcriptionally active (Figure 2B), such a result suggested that topo-I binding rather than transcriptional activation (TA) is required for p53-mediated DDT. We then tested the effect of an N-terminally truncated p53ΔN, missing aa 1 to 79 and thereby both N-terminal TA domains (TAD1: aa 1–40, TAD2: aa 40–60) (20) and found that both recombination stimulation (Figure 2A) and TA by p53 (Figure 2B) were abrogated in this p53 mutant. While this result could indicate TA dependency, it should be taken into consideration that the N-terminus also binds the single-stranded DNA (ssDNA) binding protein RPA (Replication Protein A), which stabilizes DNA replication intermediates (8,21). This domain also binds DNA polymerase beta (POLß), which shares with POLι the capacity to bypass DNA crosslinks and is involved in base excision repair (BER) (22,23). To target both binding sites individually, we expressed p53(48H/49H), which selectively disrupts RPA-binding (8) (verified by proximity ligation assay in Supplementary Figure S2C), and p53(22Q/23S), which is deficient in POLß-binding. Both mutations reduced replication-associated recombination if compared with p53(WT) (Figure 2A). This reduction in recombination-mediated events took place even under conditions of higher levels of p53ΔN or p53(22Q/23S) mutants when compared to p53(WT) (Figure 2B, Supplementary Figure S2), which may result from impaired E3 ubiquitin ligase MDM2 interaction with p53's N-terminal 40 aa caused by a disrupted N terminal sequence. Notably, cells expressing p53(22Q/23S) showed an additional 13% reduction of recombination frequencies in comparison to p53-negative control cells ($P < 0.01$, Figure 2A) suggesting a moderate gain of negative effect of this mutant.

While the above mentioned results engaging p53(315A) and p53(48H/49H) demonstrated that p53 regulates homology-directed DDT independently of its TA functions, some p53 target gene products, namely p21 and MDM2, were reported to play modulatory roles in DNA replication independently of p53 (24,25). To examine the contribution of p21 and MDM2 to p53-dependent replication-associated recombination, we re-expressed exogenous p21 and MDM2 in cells expressing TA-defective p53(22Q/23S) (Supplementary Figure S2A, B). The overexpression of either p21 or MDM2 did not re-activate recombination in p53(22Q/23S) expressing cells, indicating that neither p21 nor MDM2 were sufficient to rescue the defect of replication-associated recombination in cells expressing p53(22Q/23S) (Supplementary Figure S2A, B). Altogether these data suggest the involvement of topo-I binding and N-terminal protein interactions in the replication-associated recombination events triggered by p53.

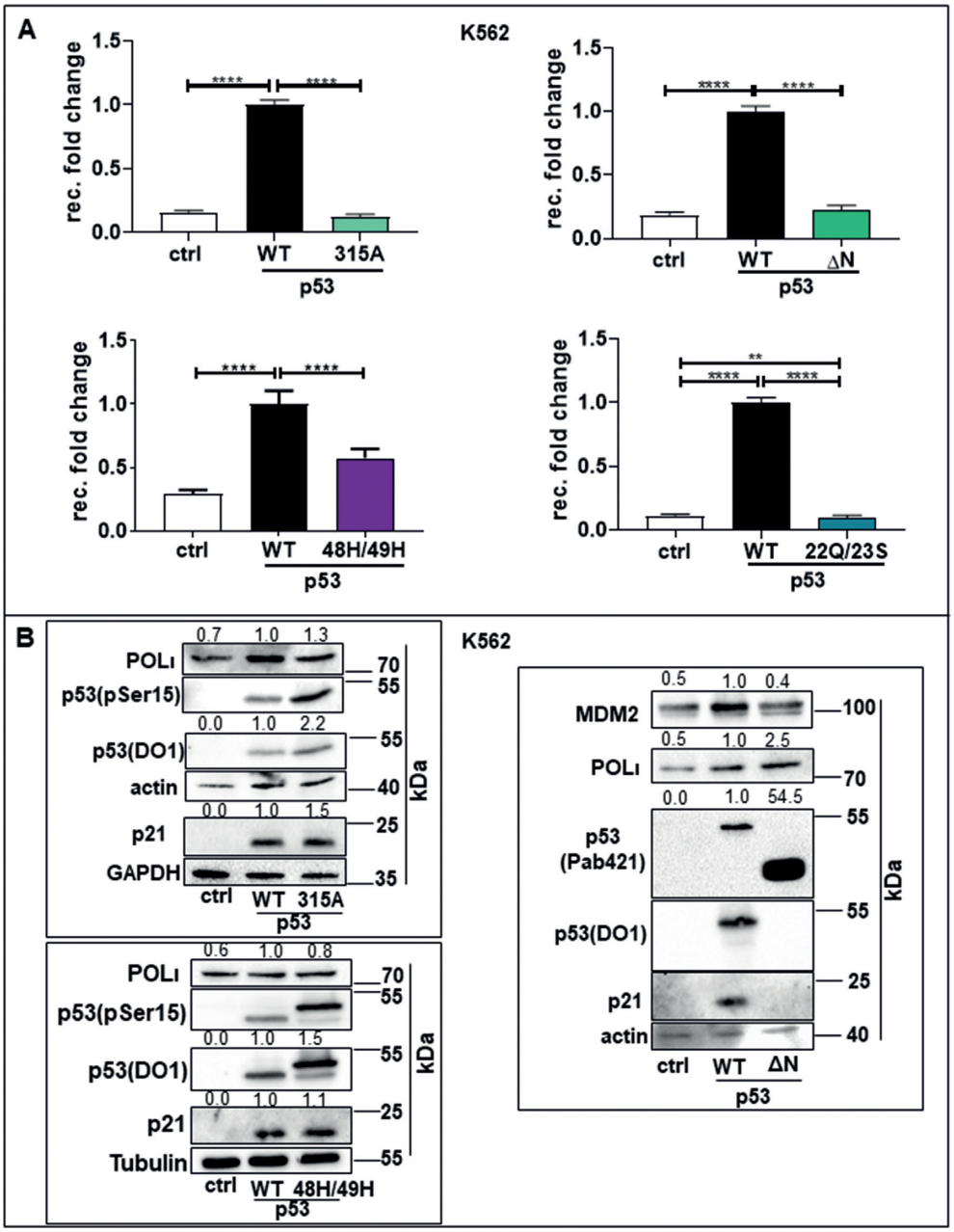

Figure 2. Effect of mutating S315 and N-terminal residues of p53 on DNA recombination. K562(HR-EGFP/3′-EGFP) (**A**) or K562 parental (**B**) cells were transfected with expression plasmids for p53(WT), p53(315A), p53(ΔN), p53(22Q/23S), p53(48H/49H) or empty vector (ctrl). 48 h (B) or 72 h (A) after transfection experiments were performed as described in Figure 1. For graphic presentation, calculation of SEM and statistically significant differences between the mean values via Kruskal–Wallis test followed by Mann–Whitney *U* test GraphPadPrism8.4 software was used. $^{**}P < 0.01$, $^{****}P < 0.0001$.

DNA replication dynamics and replication-associated recombination are similarly affected by p53 mutants 315A, ΔN, 48H/49H and 22Q/23S

To investigate the impact of the p53 mutants described above on the dynamics of nascent DNA replication, we performed DNA fiber spreading assays (see protocol in Figure 3A) in the p53-negative K562 and Saos-2 cells (Figure 3B–E, Supplementary Figure S3). Mirroring dysfunction in replication-associated recombination, experiments performed in K562 cells showed that the p53 mutants p53(315A), p53ΔN, p53(48H/49H) and p53(22Q/23S) were all impaired in the ability to limit the elongation rate of nascent DNA synthesis when compared to p53(WT) (Figure 3B–E, Supplementary Figure S3A). Similar results were observed when subjecting K562 to MMC-treatment during the second IdU pulse (Supplementary Figure S3A). Similarly, all four p53 mutants were impaired in the ability to decelerate DNA replication in Saos-2 cells during MMC treatment (Supplementary Figure S3B). Interestingly, the p53(22Q/23S) mutant which caused the most severe loss of recombination induction (Figure 2A), completely failed to slow down DNA replication in both cell

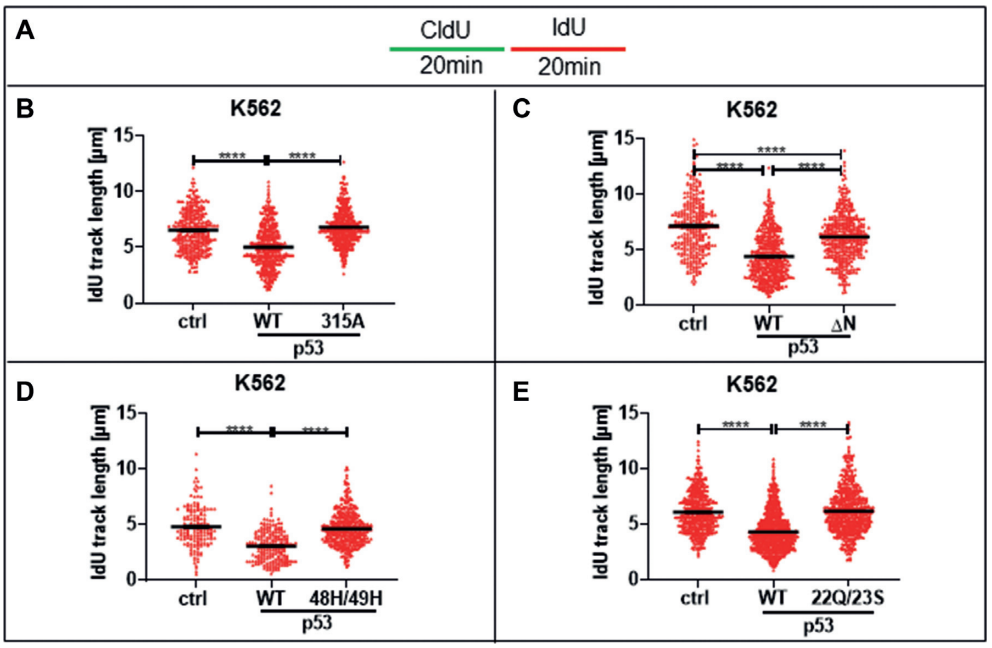

Figure 3. Effect of mutating S315 and N-terminal residues of p53 on DNA replication. (**A**) Graphic overview of the experimental outline. K562 cells were transfected with expression plasmids for (**B**) empty vector (ctrl), p53(WT) and p53(315A) or (**C**) p53(ΔN) or (**D**) p53(48H/49H) or (**E**) p53(22Q/23S). 48 h after transfection DNA fiber analysis was performed as described in Figure 1. Both CldU- and IdU-tracks were measured; only IdU-track results for ongoing forks are shown for clarity (≥163 to ≥499 fibers in two independent biological experiments). For graphic presentation, calculation of SEM and statistically significant differences via Dunn's multiple comparison test GraphPadPrism8.4 software was used. ****$P < 0.0001$. Only statistically significant differences ≥0.0001 are shown. Bars indicate mean values.

lines with and without MMC treatment as well as in H1299-cell clones inducibly expressing p53(22Q/23S) (Supplementary Figure S3C). For comparison, p53(315A), p53ΔN and p53(48H/49H) showed a moderate but yet significant residual decelerating activity at least under one of the conditions each. For example, in untreated K562 cells the fork rates (FR) were reduced from 0.95 kb/min in p53-negative controls to 0.80 kb/min in p53ΔN expressing cells, which was significantly above the p53(WT)-specific FR of 0.57 kb/min. During MMC exposure in K562 cells p53(48H/49H) expression caused intermediate track shortening with a fork rate of 0.51 kb/min (compared to controls: FR = 0.61 kb/min or p53(WT) expressing cells: FR = 0.38 kb/min). In MMC-treated Saos-2 cells expressing p53(315A) the replication speed was FR = 0.56 kb/min versus controls (FR = 0.66 kb/min) and p53(WT) (FR = 0.38 kb/min). Altogether, these data demonstrate that loss of the integrity of these critical protein interaction sites in p53 compromises its ability to slow nascent DNA synthesis. Given the association of shorter tracks with the p53-POLι-dependent DDT pathway (3), these results suggest that these p53 mutants are impaired in this pathway at forks encountering obstacles. Yeo *et al.*, 2016 demonstrated that HCT116 cells devoid of p53 show increased topological conflict between transcription and replication complexes (transcription-replication conflict, TRC) (26). To see if the use of a transcription inhibitor influences the effect of p53 on the p53-POLι DDT pathway, we (pre-)treated H1299-cells with the inhibitor 5,6-dichlorobenzimidazone-1-β-D-ribofuranoside (DRB) (26). DNA fiber spreading analysis revealed a shortening of track lengths both after p53 induction and after DRB-treatment (Supplementary Figure S4). Interestingly, we still noticed residual p53-mediated shortening of the tracks in the presence of DRB, suggesting that the p53-POLι DDT pathway may be triggered by transcription-dependent and -independent replication obstacles.

p53 mutants 315A, ΔN, 48H/49H and 22Q/23S are impaired in protecting cells from DNA damage accumulation

p53-mediated homology-directed DDT, which helps to overcome replication barriers (3), could mitigate the accumulation of replication stress, revealed as the accumulation of H2AX phosphorylated on serine 139 (γH2AX) (27,28). To assess the impact of the different p53 mutants on DNA damage accumulation, we performed immunofluorescence microscopy to detect γH2AX foci 24 h after treatment of Saos-2 cells with the DNA interstrand crosslinker MMC. DNA interstrand crosslinks generate roadblocks for DNA replication (29,30), and are therefore a potent inducer of γH2AX in replicating cells as confirmed in Figure 4. In support of the notion that p53(WT) protects cells from replication damage, γH2AX foci numbers were 2- to 3-fold lower in p53(WT) expressing Saos-2 cells in comparison to p53-negative cells (Figure 4A–D). The p53-mutants p53(315A), p53ΔN and p53(48H/49H) lost the ability to restrain γH2AX foci numbers in comparison to p53(WT) expressing cells, displaying levels of foci accumulation which were similar to those of p53-negative cells (Figure 4). The expression of p53(22Q/23S) induced intermediate DNA damage levels, i.e. less γH2AX foci accumulation as in p53-

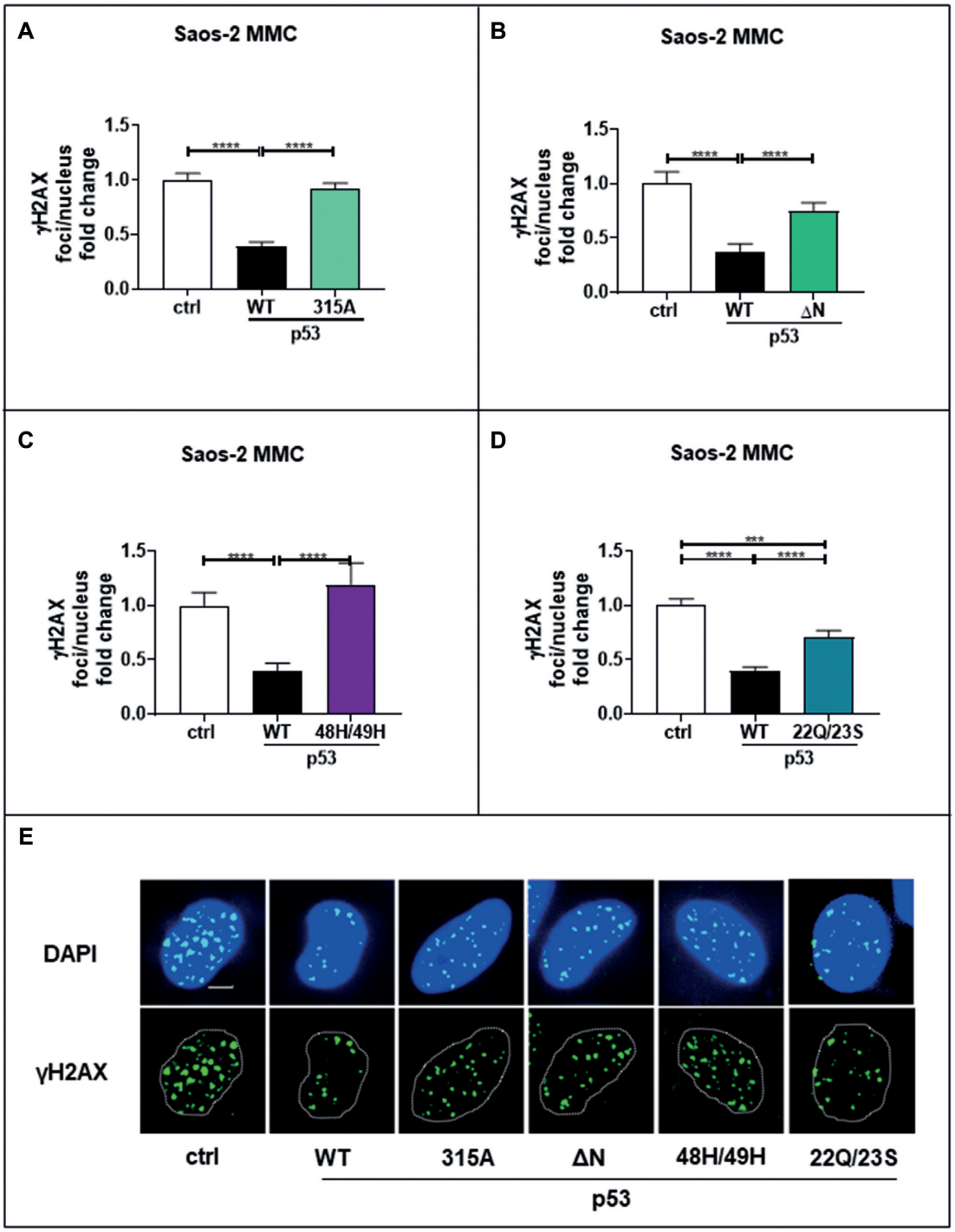

Figure 4. Analysis of DNA damage in cells expressing different p53 mutants. (A–E) Saos-2 cells were transfected with expression plasmids for p53(WT), empty vector (ctrl) or the respective p53 mutants (**A**) p53(315A), (**B**) p53(ΔN), (**C**) p53(48H/49H), (**D**) p53(22L/23W). 24 h after transfection cells were MMC-treated (3 μM, 45 min, 24 h release) and processed for immunostaining to visualize γH2AX-foci. The experiments of (A) and (D) as well as (B) and (C) were performed together: Columns of ctrl and p53(WT) are identical. Mean values of ctrl expressing cells were set to 1 (on average 3 [A, D] or 45 [B, C] foci per nucleus). ≥127 nuclei (A, D) and ≥125 nuclei (B, C) were scored in two independent experiments. For graphic presentation (left panel), calculation of SEM and statistically significant differences via Dunns multiple comparison test GraphPadPrism8.4 software was used. ***$P < 0.001$, ****$P < 0.0001$. (**E**) Representative images with γH2AX-foci and merged images with a DAPI-stained nucleus are shown (Scale bar: 5 μm).

negative cells but still higher than in p53(WT) expressing cells (Figure 4D). These data demonstrate that p53 mutants, which fail to decelerate the replication elongation rate, are deficient in protecting cells from the accumulation of replication-associated DNA damage.

Stable complex formation of p53 and POLι at the replication fork requires the integrity of p53′s N-terminus

To investigate why the p53 mutants p53(315A), p53ΔN, p53(48H/49H) and p53(22Q/23S) have lost the capacity to protect cells from DNA damage, achieve replication-associated recombination and restrain nascent DNA replication, we explored the ability of these mutants to associate with key DDT players discovered in our preceding work (3). To this end, we performed *in situ* proximity ligation assays (PLA) to explore the association of PCNA, POLι and p53 in K562 cells (Figure 5). To detect p53 we used the antibody against p53 phosphorylated on Serine 15 (p53pSer15) which recognizes all p53 mutants including p53(22Q/23S) except for p53ΔN (Supplementary Figure S5). In case of p53ΔN, devoid of Serine 15, we used the antibody p53 (Pab421) against the C-terminus of p53. When exploring the association of p53(WT) with PCNA in the nucleus, p53(315A), p53ΔN, p53(48H/49H) and p53(22Q/23S) showed a 75% to 100% reduction in PLA-foci numbers in comparison to p53(WT) expressing cells (Figure 5A). Notably, p53(48H/49H) revealed the most dramatic (100%) impairment followed by p53ΔN (88%), p53(22Q/23S) (75%) and p53(315A) (74%). Corresponding PLA analysis of p53-POLι associations showed the most pronounced impairment of p53(315A) (95%), followed by p53(48H/49H) (81%), p53ΔN (81%) and p53(22Q/23S) (64%) (Figure 5B). Finally, we interrogated the impact of the different p53 mutants on the association of POLι with PCNA. Analysis of PCNA-POLι PLA signals showed that p53(WT) increased the association of POLι with PCNA 4.3 to 10.4-fold, whereas all other p53 mutants were significantly impaired (Figure 5C).

Similarly, when analyzing PCNA–POLι complex formation in co-localization studies, we detected a 11- to 15-fold stimulation of POLι association with PCNA upon expression of p53(WT) but not after expression of the p53 mutants in K562 cells (Supplementary Figure S6A). Similar results were obtained in Saos-2 cells (Supplementary Figure S6B) On average 19% of all POLι and 23% of all PCNA foci overlapped with each other in p53(WT) expressing K562 cells, and 20% of all PCNA or POLι foci overlapped with each other in p53(WT) expressing Saos-2 cells. Strikingly, the relative degree of impairment of inducing PCNA-POLι complex formation was similar for the different mutants in both cell lines (see heatmaps in Supplementary Figure S6A and B). In particular, in both cellular backgrounds, the mutation of aa 22–23 or the deletion of aa 1–79 (ΔN) in p53 caused the most severe defects in the colocalization of POLι with PCNA (Supplementary Figure S6). A similar, yet less pronounced pattern, was also seen for POLι foci formation in both cell lines, possibly reflecting mutual stabilization of p53 and POLι at replication factories, e.g. in the idling complexes (3). PCNA foci numbers showed smaller variations than seen for PCNA-POLι colocalization in both cell lines, particularly in Saos-2 (Supplementary Figure S5). Altogether, recruitment of POLι to PCNA-labeled DNA replication sites was dependent on the p53 functions abrogated in these p53 mutants, whereby mutating aa 22 and 23 caused the most severe defect.

Since both POLι and PCNA are involved in base excision repair (BER), we also investigated if some foci were also BER-related foci (31–33). To this end, we performed a PLA experiment after H_2O_2 to explore the association between the BER factor X-Ray Repair Cross Complementing 1 (XRCC1) and POLι under conditions of oxidative stress (Supplementary FigureS7A). Similar to Petta *et al*., we also observed here, in H1299-cells, that POLι associates with XRCC1 particularly after H_2O_2-treatment (33). A similar PLA-foci augmentation was observed under conditions inducing p53-POLι PLA foci, i.e. when treating samples with the crosslinker MMC (3). However, the number of XRCC1–POLι PLA foci was not significantly affected by p53 expression. Consistently, a rise in PLA foci number also revealed that another BER enzyme, Apurinic/Apyrimidinic Endodeoxyribonuclease 1 (APE1), and POLι are in close proximity to each other (Supplementary Figure S7B). However, the expression of p53 suppressed APE1–POLι PLA foci numbers almost to the basal level after both H_2O_2- and MMC-treatment. These data suggest that p53(WT), instead of promoting the BER function of POLι, rather antagonizes the association of POLι with BER factors.

Given that the N-terminus of p53 was already suggested to be a potential binding site for polymerases and that p53(22Q/23S) showed the most severe defects of the investigated p53 mutants in this study, we investigated p53(22Q/23S) in terms of its physical interaction with POLι in co-immunoprecipitation experiments in K562 cells. As reported before (3), p53(WT) and POLι were pulled-down in immunoprecipitations (Figure 6). Very differently, p53(22Q/23S) was not detected in POLι immunoprecipitations done in parallel (Figure 6). We obtained similar results when using the PLA approach: no association between p53 and POLι was observed (Figure 5B). These results suggest that mutating the residues L22/W23 disrupts the interaction of the two main proteins in the DDT complex (p53 and POLι) at damaged fork sites.

DISCUSSION

Recently, we described a novel homology-directed DDT pathway that requires the combined action of POLι and p53 to decelerate nascent DNA elongation at replication barriers, suggesting idling events facilitating their resolution by fork reversal (3). Moreover, DNA-replication-dependent, spontaneous recombination events of a genomic integrated GFP-based recombination reporter provide an independent read-out of the DDT pathway. In this work, we define the biochemical features of the p53 molecule that are prerequisites for the resolution of replication barriers in concert with POLι. Collectively, our data suggest that p53 mediated DDT across replication barriers involves: (i) p53 DNA binding in its tetrameric configuration and (ii) physical interactions with key proteins in the pathway. Moreover, by using separation-of-function mutants we provide evidence that this function is independent of its TA activity. Dissec-

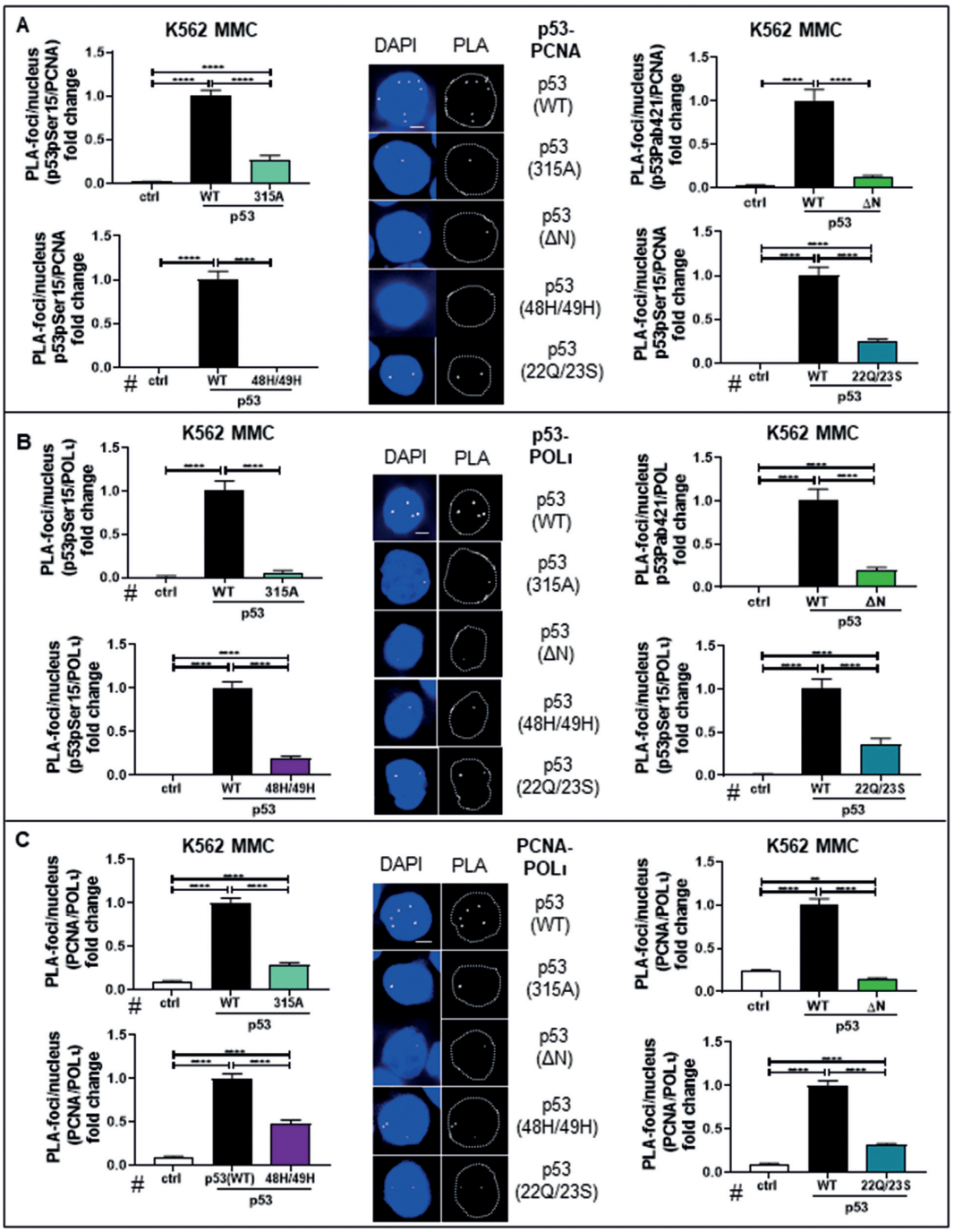

Figure 5. Identification of POLι–PCNA complex partners in cells expressing different p53 mutants. K562 cells were transfected with expression plasmids for p53(WT), p53(315A), p53(ΔN), p53(48H/49H), p53(22Q/23S) or empty vector (ctrl). 48h after transfection cells were MMC-treated (3 μM, 45 min, 3 h release) and PLA performed. For graphic presentation of mean values, calculation of SEM and statistically significant differences via Dunns multiple comparison test GraphPadPrism8.4 software was used. $^{**}P < 0.01$, $^{***}P < 0.001$, $^{****}P < 0.0001$. Representative images with PLA-foci and merged images with a DAPI-stained nucleus are shown (Scale bar: 5μm). Hashtags indicate experiments were performed together: Columns of ctrl and p53(WT) are identical. (**A**) Association of p53 with PCNA was analyzed by *in situ* PLA using primary antibodies against p53 and PCNA. Note that for immunodetection of p53(315A), p53(48H/49H) and p53(22Q/23S) anti-p53pSer15 and for detection of p53(ΔN) devoid of serine 15 Pab421 were applied. Mean values of p53(WT) expressing cells were set to 1 (on average seven foci per nucleus), ≥100 nuclei were scored in two independent experiments. (**B**) Association of p53 and POLι by PLA was performed using primary antibodies against p53 as in (A) and against POLι. Mean values of p53(WT) expressing cells were set to 1 (on average four foci per nucleus) ≥141 nuclei were scored in two independent experiments. (**C**) Association of PCNA and POLι by PLA was performed using primary antibodies against PCNA and POLι. Mean values of p53(WT) expressing cells were set to 1 (on average four foci per nucleus), ≥233 nuclei were scored in two independent experiments. Bars indicate SEM.

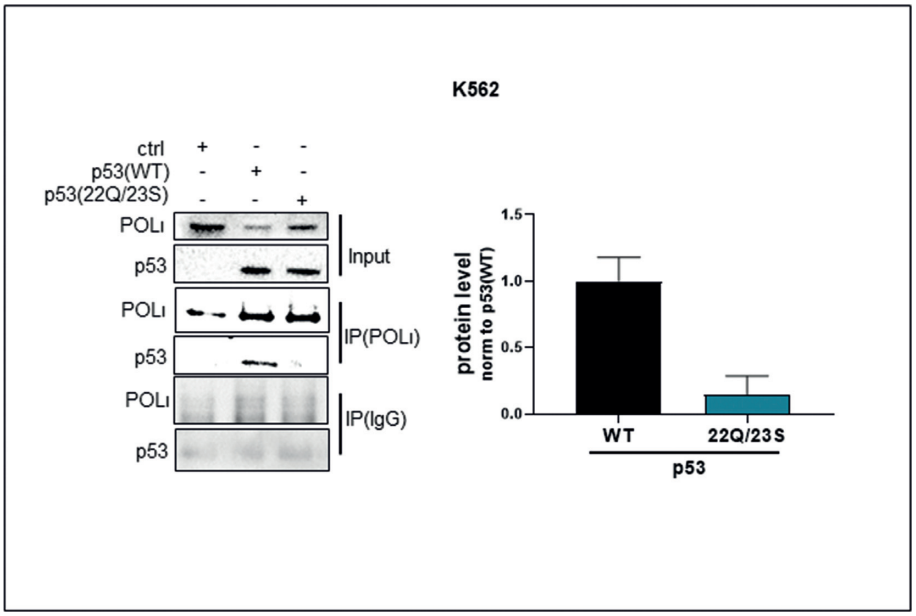

Figure 6. p53's N-terminus as binding partner for POLι. K562 cells were transfected with expression plasmids for p53(WT), p53(22Q/23S) or empty vector (ctrl). Immunoprecipitations were performed 48 h after transfection. Pull-downs engaged polyclonal rabbit POLι-antibody (Bethyl, A301–304A) or control rabbit IgG, subsequent immunoblotting relied on anti-POLι, anti-p53 (mix of mAbs Pab421 and DO1) and light chain-specific peroxidase-coupled secondary antibody. The left panel shows a representative Western Blot. The right panel shows the quantification of three immunoprecipitations. Quantification of p53 was carried out with ImageLab software and corrected for values of the pull-down protein POLι, whereby the mean value for p53(WT) samples was set to 1. Mean ±SD. Note, that the values of the ctrl were subtracted from the values of p53(WT) and p53(22Q/23S). Due to the small number of values (n = 3) no statistical significant differences were achieved when comparing p53(WT) to p53(22Q/23S) or ctrl. IP = Immunoprecipitation of POLι.

tion of the key interaction sites of p53 necessary for DDT resolution of replication barriers provides evidence for involvement of S315, which was reported to target topo-I for recruitment to replication-associated DNA lesions (16). Residues D48 and D49 which were described to be required for the p53-RPA interaction (8) and L22 and W23 required for POLι complex formation (this work) are also central for p53-mediated DDT.

DNA binding is necessary for DDT mediated by p53 in concert with POLι

The p53 tetramer cooperatively binds to palindromic TA target DNA in a sequence-specific fashion (34,35) as well as to Holliday junctions and three-stranded junctions in a secondary structure-specific fashion (36,37). We presumed that for p53 to act in DDT, cooperative DNA binding to such junctions after fork disturbance might be necessary. Compatible with our idea, we observed that the cancer-related mutants p53(248W) and p53(273H), which have lost the capability to contact the phosphate backbone in the DNA (38), neither stimulate replication-associated recombination nor decelerate nascent DNA elongation. Therefore, we concluded that p53 needs its DNA binding core domain to perform DDT. Moreover, mutant p53ΔO missing aa 327–346, i.e. the oligomerization domain, also showed complete loss-of-DDT function. This observation demonstrates that high-affinity binding of p53 to the replication sites requires p53 tetramerization, which is compatible with multiple cooperative DNA binding site at the disturbed replication fork three-way junctions (39). While the core domain rather stochastically associates and dissociates from the DNA, p53 slides in a sequence-independent manner on DNA via its C-terminal domain (40). Interestingly, lack of the aa 370–393 rather enhanced the bypass activities of p53 in the DDT pathway, as we observed hyperstimulation of replication-associated recombination by p53ΔC. Intriguingly, we also noticed levels of PCNA-ubiquitination above p53(WT), which like recombination was the opposite of the loss-of-function phenotype of the core domain and oligomerization mutants (Supplementary Figure S8). The intrinsic 3′-5′ exonuclease activity of p53 was previously suggested to regulate PCNA ubiquitination (41). The enhanced homology-directed DDT phenotype of p53ΔC may therefore result from the reported de-repression of the 3′-5′ exonuclease activity of p53 after the deletion of the C-terminus (42). The coordinated exonuclease and polymerase activities of p53-POLι complexes were suggested to cause idling events (3). These iterative processes may open a window of opportunities for PCNA-ubiquitination by HLTF and DDT fork reversal by ZRANB3. As a consequence, homology-directed DDT is critically influenced by two p53-dependent steps: (i) p53-POLι-mediated idling which gives time for enhanced PCNA-mono- and poly-ubiquitination by HLTF (3,43) and (ii) ZRANB3-mediated fork reversal, which initiates the homology-directed annealing of the two nascent strands to form a chicken foot structure. These observations suggest that efficient recruitment of p53 to DNA seems to play a determinant role in the regulation of homology-directed DDT. Recruitment of p53 to DNA was also essential for the slow-down of the DNA replication dynamics, while the influence of the C-terminus was minor. Altogether, p53-mediated DDT in concert with POLι requires the integrity of the core domain harboring

both DNA binding and exonuclease activities as well as the oligomerization domain.

During POLι–dependent DDT, the recruitment of p53 to replication forks relies on its interaction with topo-I and RPA

Having established the relative importance of cooperative DNA binding by a p53 tetramer, we investigated the hierarchy of p53 interactions with DNA binding proteins in the p53-POLι DDT pathway utilizing previously described loss of function mutations of p53 (Figure 7). In our previous works we were intrigued by the fact that p53-dependent replication-associated recombination requires stable complex formation of p53 with topo-I (16). Topo-I is an enzyme known to release torsional stress created by transcription and replication processes on the DNA double helix (44). In order to generate a p53–topo-I complex, S315, which is positioned between the core domain and the OD of p53, must be phosphorylated by CDK2 in complex with Cyclin A1 (16) Cyclin A1 expression accelerates S phase entry (45), which suggested a role of the p53–topo-I complex during DNA replication. Consistent with the notion that recruitment of p53 to replication sites via topo-I binding is a prerequisite for initiation of p53–POLι-mediated DDT, we found complete loss of essential biochemical activities underlying this pathway upon mutating S315 in p53 (Figure 7): Notably, while stimulation of replication-associated recombination, DNA replication track shortening and association between p53, POLι and PCNA were lost when expressing p53(315A), this mutant is fully active in DNA binding and TA. p53(315A) was the mutant with the worst performance when evaluating associations between p53 and POLι molecules in the nucleus. Therefore, recruitment of p53 by topo-I must be an upstream prerequisite in the p53-POLι-mediated DDT pathway (Figure 7), possibly by releasing tension introduced by p53 to the multiple sites around the disturbed fork.

As noticed almost three decades ago, both wild-type and oncogenic mutant p53, physically interact with RPA in S-phase via residues 38–58 located within the N-terminus (46). RPA is the major human ssDNA binding protein during DNA replication, and promotes the assembly of several factors involved in DNA replication and repair. RPA is formed by three subunits and the largest one, RPA70, can be further subdivided into four domains, of which RPA70A/B/C bind to ssDNA and RPA70N serves as an interaction partner for other proteins including p53. Therefore, p53 may be recruited to replication sites via RPA (47). RPA interacts with the N-terminus p53, and the p53(48H/49H) mutant was shown to be deficient in RPA binding (8). However, RPA binding to ssDNA and to p53 seem to be mutually exclusive which has led to the idea that ssDNA, which is enriched at DNA lesions and replication forks encountering such obstacles, can trigger dissociation of the p53-RPA complex, shown by less p53–POLι, p53–PCNA or PCNA–POLι association *in situ* in p53(48H/49H) expressing cells compared to p53(WT) cells detected by our PLA study (Figure 5). Hence, RPA may aid the recruitment of p53 to replication sites, while RPA dissociation from the ssDNA lesion might release p53 for new functions in modulating nascent DNA elongation (48). At PCNA sites, p53 binds DNA together with POLι initiating idling events which further stabilizes the ternary complex between p53, POLι and PCNA. On the other hand, in comparison to all other investigated p53 mutants, p53(22Q/23S) showed the most severe defect in replication track shortening, as it has lost the most crucial prerequisite, namely the physical binding of p53 to POLι (Figure 7).

Physical interactions of p53 with POLι specifically require L22 and W23 within the N-terminus

In our previous work, we showed that a p53 mutant p53(115N), which is TA-proficient but exonuclease-deficient was deficient in stable p53–POLι idling complex formation, track shortening and recombination stimulation (3). These findings suggested that p53 directly acts in this DDT pathway rather than via effects of its downstream targets. In our work presented here, two additional separation-of-function mutant proteins, p53(315A) and p53(48H/49H), provided further evidence for a direct role of p53 in this DDT mechanism. We also observed that p53(22Q/23S), originally reported to be impaired in TA via loss of the interactions with TFIID and TFIIH components (17), does not any longer show interaction with POLι in co-immunoprecipitation, and strongly reduced association with POLι and PCNA *in situ* studied by PLA. Consistently, p53(22Q/23S) is inactive in p53-POLι-dependent DDT pathway functions. Of note, p53(22Q/23S) is also impaired in binding to POLβ, mouse double minute protein 2 (MDM2 or HDM2 in humans) and adenovirus E1B (9,49). These findings suggested that p53's N-terminus also harbors binding-sites for other proteins than transcription factors and therefore mediates biochemical activities other than TA.

MDM2 antagonizes p53's TA function through competitively inhibiting access of the transcription machinery to the N-terminal TAD. Additionally, it down-regulates p53′s protein level by inducing ubiquitination followed by proteasomal degradation (50–52). Interestingly, it was also reported that MDM2 has a p53-independent role in regulating replication processes by chromatin remodeling (53). p21 also has p53-independent roles in DDT as a key regulator of TLS (54). However, here we provide data indicating that re-expression of p53′s transcriptional target gene products MDM2 and p21 in cells expressing TA-defective p53(22Q/23S) do not reconstitute the replication-associated recombination phenotype of p53(WT) cells. In this context, it is also of interest that our PLA studies demonstrating association between p53–POLι, p53–PCNA or PCNA-POLι *in situ*, i.e. between the key components of the DDT pathway, implied use of antibodies directed against p53pSer15 except when investigating p53ΔN functions. It is well known that phosphorylation of p53 on serine 15 alleviates MDM2 binding to p53′s N-terminus (55,56), so that altogether it is unlikely that MDM2 plays an essential role in the p53-POLι mediated-DDT pathway. In agreement with our findings, previous work had suggested that after replication fork stalling, p53pSer15 may serve additional functions unrelated to TA. Therefore, we pro-

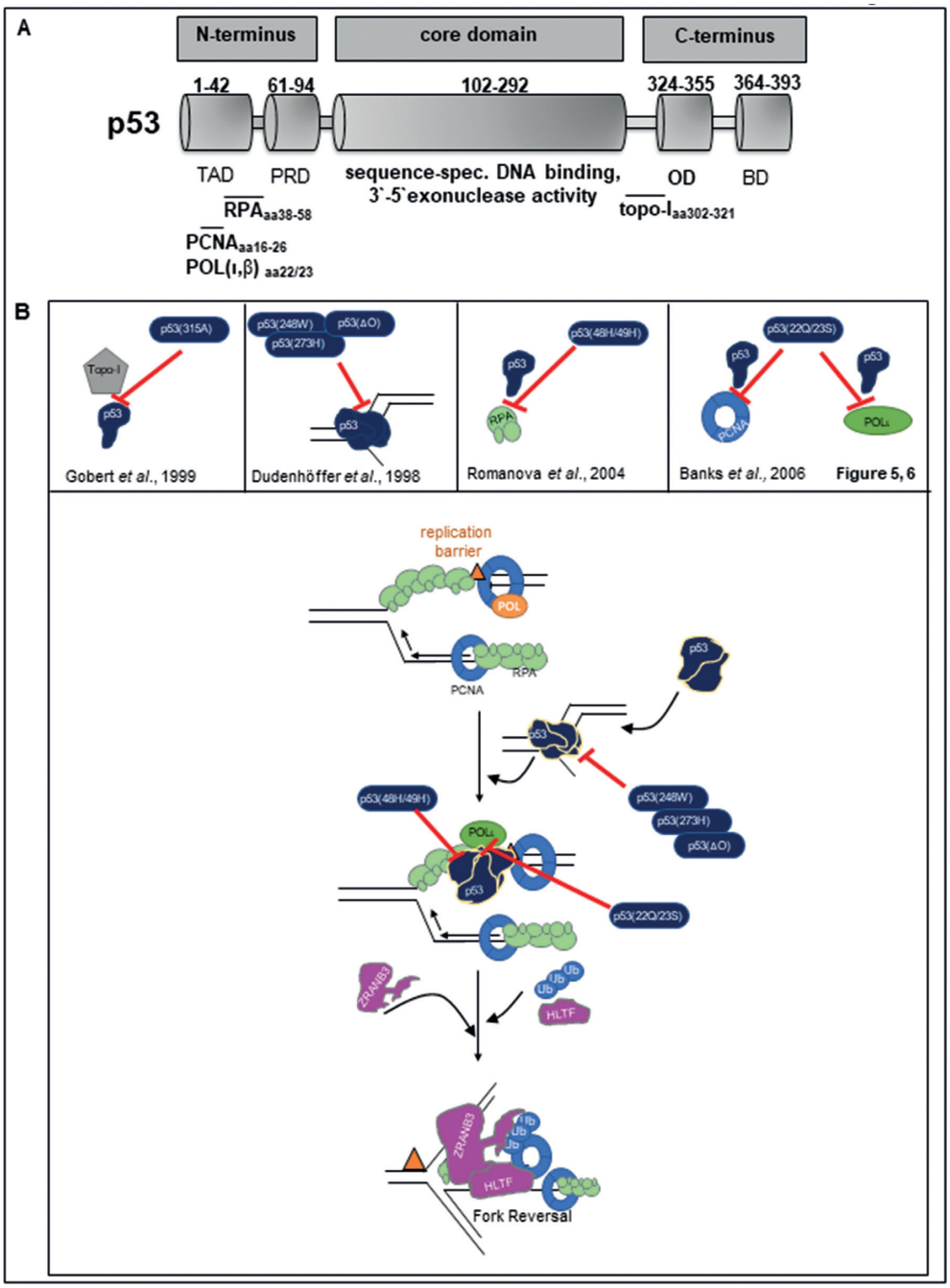

Figure 7. Hierarchy of p53's biochemical properties necessary for the regulation of DNA replication fork progression in concert with POLι. (**A**) Schematic structure of the p53(WT) protein as detailed in the text: p53(WT) consists of three main domains (N-terminus, core domain, C-terminus). The N-terminus can be sub-divided into the transactivation domain (TAD) and proline rich domain (PRD). The C-terminus can be sub-divided into the tetramerization domain (TD) and the basic domain (BD). Relevant functions of p53 (binding to three-stranded junctions in a secondary structure-specific fashion (36) or 3′-5′exonuclease activity (3)) and interaction sites [PCNA: (58), RPA: (8), Topo-I: (19)] for our study are highlighted below. (**B**) The upper panel shows p53-mutants used in this study and having been described for disrupting the binding to three-stranded junctions or the interaction with relevant proteins in the p53–POLι–DDT pathway. The p53–POLι interaction has newly been described in this work (Figures 5, 6). Red lines indicate abrogation of p53's interactions by the indicated mutations. In the lower panel we propose the following hierarchy of events in the p53–POLι–DDT pathway summarizing p53's biochemical properties necessary for the regulation of DNA replication fork progression in concert with POLι. DNA replication barriers (orange triangle) perturb the progression of the DNA replication fork, triggering the p53–POLι DDT (18). Disruption of p53's interaction with topo-I in p53(315A) (16,19) prevents the localization of this mutant to the perturbed fork, possibly as topo I might be trapped at the perturbed fork. Stable DNA binding of p53 in tetramers, lost in mutants p53(248W), p53(273H) and p53(ΔO), is necessary for prolonged association with DNA replication sites (36,39). Moreover, interactions of p53 with RPA target p53 to ssDNA at these replicating sites (Supplementary Figure S2C, Figure 5), increasing the specificity for localization at perturbed forks (Figures 1D, 3). Consequently, the RPA-binding defective p53(48H/49H) is impaired in the DDT pathway (Figure 5). Being located at the replication sites, p53–POLι perform perpetual nucleotide incorporation and removal steps (3) (Figures 1D, 3), which further stabilizes the ternary p53–POLι–PCNA complex. Moreover, this gains time for PCNA poly-ubiquitination (Supplementary Figure S8) and subsequent HLTF-ZRANB3 mediated fork reversal and restart (3,60,61).

pose that p53 residues 22 and 23 supported biochemical activities other than MDM2 binding or TA, e.g. p53–POLι complex formation during the p53-POLι dependent DDT. Zhou *et al*. reported that residues 22 and 23 are the binding site for another polymerase, namely POLß. As p53 is involved in several DNA repair pathways (57) it is tempting to speculate that the N-terminus of p53 is important for several processes other than TA, including interactions with DNA polymerases. Supporting this concept, also the DNA polymerase platform PCNA was described to interact with aa 16 to 26 of p53 (58). In conclusion, our data together with the wealth of information on p53 functions suggest a highly coordinated mechanism of p53-dependent DDT (Figure 7): p53-POLι associates with disturbed replication forks dependent on its oligomeric state, cooperative DNA binding and interaction with Topo-I. This is further assisted by interaction with RPA and (ubiquitylated) PCNA. This then leads to formation of a ternary p53-POLι-PCNA complex, and the suggested idling to buy time for PCNA polyubiquitylation and subsequent HLTF-ZRANB3 mediated fork reversal (3,4).

Protection from replication stress

Our previous studies suggested that the p53–POLι DDT pathway protects quickly growing cancer and stem cells from replication stress which implicated a pro-survival function of p53(WT) (3). Thus, inactivation of endogenous p53(WT) was linked to a decrease of replication-associated recombination, reduced survival in response to PARP-inhibitor treatment as well as an increase in spontaneous and treatment-induced γH2AX foci (2). In our study presented here, we demonstrated that p53(WT) reduced the accumulation of γH2AX foci after MMC-induced replication stress, but mutants p53(315A), p53(ΔN), p53(48H/49H) or p53(22Q/23S) were impaired in this ability. These results provide further evidence that the p53–POLι DDT pathway protects against the accumulation of DNA damage. Mutant p53(22Q/23S) was different than other p53 mutants, as it showed the milder reduction in γH2AX but a strong reduction in replication-associated recombination which was significantly lower than the levels of replication-associated recombination of p53-negative cells. Such a gain-of-negative function effect could be caused by the formation of unproductive complexes between p53(22Q/23S) and factors such as topo-I or RPA thereby exacerbating the DDT problem by sequestering key molecules away from replicative DNA. In this scenario, the DDT pathway choice may also have a contribution as TLS can antagonize recombination resulting from fork reversal and thus modulating the levels of γH2AX foci indirectly. Such a DDT pathway choice should affect DNA replication fidelity. Hence p53 may be crucial to direct POLι into a genome stabilizing p53–POLι DDT pathway versus in highly mutagenic TLS choice. Supporting such notion, knockout mice for POLι unexpectedly revealed tumor suppressor functions that were interpreted to be separate from its role as a TLS polymerase (59). Therefore, the p53(WT) mediated DDT may contribute to the tumor suppressor functions of both p53 and POLι.

DATA AVAILABILITY

The datasets generated during and/or analyzed during the current study are available from the corresponding authors upon request.

SUPPLEMENTARY DATA

Supplementary Data are available at NAR Online.

ACKNOWLEDGEMENTS

We would like to thank the Wiesmüller laboratory for constant support and Michaela Ihle as well as Galina Selivanova and Jiawei Zhu for enlightening discussions. We thank Manuel Seedorfer and Rahel Fietze for helping with experimental work during a 4-weeks internship and performed experiments together with SB. We are grateful to Klaus Römer (Homburg/Saar, Germany) for the generous gifts of vectors pCMV-p53(WT), pCMV-p53(ΔN), pCMV-p53(ΔO), pCMV-p53(ΔC) and pCVM-p53(22Q/23S) and to Carol Prives (New York, USA) for providing the isogenic cell lines H1299-p53(WT), H1299-p53(248W) and H1299-p53(22Q/23S).
Authors contributions: L.W. conceived the study, S.B. and L.W. designed the experiments. S.B. performed the experiments and processed the data, S.B. and L.W. interpreted the data with the help of H.P. and V.G., L.W. designed the manuscript flow with the help of S.B., V.G. and H.P.; S.B. and L.W. designed the figure flow and S.B. generated the figures and wrote the initial draft of the manuscript. All authors edited the manuscript and agreed to this description of the author's contributions.

FUNDING

German Cancer Aid, Priority Program 'Translational Oncology' [70112504]; Deutsche Forschungsgemeinschaft (DFG, Research Training Group) [2544 to L.W.]; German Research Foundation (DFG) Graduate School of Molecular Medicine, Ulm University (PhD fellowship to S.B.) as well as the Start-up Funding Program of the Medical Faculty of Ulm University ('Bausteinprogramm') [L.SBN.0160 to S.B.]; V.G. was supported by the Alexander von Humboldt Foundation during her extended stay in the Wiesmüller laboratory (Georg Forster Award to V.G.). Funding for open access charge: DFG and German Cancer Aid.
Conflict of interest statement. None declared.

REFERENCES

1. Pilzecker,B., Buoninfante,O. and Jacobs,H. (2019) DNA damage tolerance in stem cells, ageing, mutagenesis, disease and cancer therapy. *Nucleic Acids Res.*, **47**, 7163–7181.
2. Ireno,I.C., Wiehe,R.S., Stahl,A.I., Hampp,S., Aydin,S., Troester,M.A., Selivanova,G. and Wiesmüller,L. (2014) Modulation of the poly (ADP-ribose) polymerase inhibitor response and DNA recombination in breast cancer cells by drugs affecting endogenous wild-type p53. *Carcinogenesis*, **35**, 2273–2282.
3. Hampp,S., Kiessling,T., Buechle,K., Mansilla,S.F., Thomale,J., Rall,M., Ahn,J., Pospiech,H., Gottifredi,V. and Wiesmüller,L. (2016) DNA damage tolerance pathway involving DNA polymerase ι and the tumor suppressor p53 regulates DNA replication fork progression. *PNAS*, **113**, E4311–E4319.

4. Weston,R., Peeters,H. and Ahel,D. (2012) ZRANB3 is a structure-specific ATP-dependent endonuclease involved in replication stress response. *Genes Dev.*, **26**, 1558–1572.
5. Joerger,A.C. and Fersht,A.R. (2008) Structural biology of the tumor suppressor p53. *Annu. Rev. Biochem.*, **77**, 557–582.
6. Baugh,E.H., Ke,H., Levine,A.J., Bonneau,R.A. and Chan,C.S. (2017) Why are there hotspot mutations in the TP53 gene in human cancers? *Cell Death Differ.*, **25**, 154–160.
7. Chen,J., Marechal,V. and Levine,A. (1993) Mapping of the p53 and mdm-2 interaction domains. *Mol. Cell. Biol.*, **13**, 4107–4114.
8. Romanova,L.Y., Willers,H., Blagosklonny,M.V. and Powell,S.N. (2004) The interaction of p53 with replication protein A mediates suppression of homologous recombination. *Oncogene*, **23**, 9025–9033.
9. Lin,J., Chen,J., Elenbaas,B. and Levine,A. (1994) Several hydrophobic amino acids in the p53 amino-terminal domain are required for transcriptional activation, binding to mdm-2 and the adenovirus 5 E1B 55-kD protein. *Gene Dev*, **8**, 1235–1246.
10. Kamada,R., Toguchi,Y., Nomura,T., Imagawa,T. and Sakaguchi,K. (2016) Tetramer formation of tumor suppressor protein p53: Structure, function, and applications. *Biopolymers*, **106**, 598–612.
11. Weinberg,R.L., Veprintsev,D.B. and Fersht,A.R. (2004) Cooperative binding of tetrameric p53 to DNA. *J. Mol. Biol.*, **341**, 1145–1159.
12. Gatz,S.A. and Wiesmüller,L. (2006) p53 in recombination and repair. *Cell Death Differ.*, **13**, 1003–1016.
13. Fischbach,A., Krüger,A., Hampp,S., Assmann,G., Rank,L., Hufnagel,M., Stöckl,M.T., Fischer,J.M.F., Veith,S., Rossatti,P. *et al.* (2017) The C-terminal domain of p53 orchestrates the interplay between non-covalent and covalent poly(ADP-ribosyl)ation of p53 by PARP1. *Nucleic Acids Res.*, **46**, 804–822.
14. Akyüz,N., Boehden,G.S., Süsse,S., Rimek,A., Preuss,U., Scheidtmann,K.-H. and Wiesmüller,L. (2002) DNA substrate dependence of p53-Mediated regulation of Double-Strand break repair. *Mol. Cell. Biol.*, **22**, 6306–6317.
15. Schindelin,J., Arganda-Carreras,I., Frise,E., Kaynig,V., Longair,M., Pietzsch,T., Preibisch,S., Rueden,C., Saalfeld,S., Schmid,B. *et al.* (2012) Fiji: an open-source platform for biological-image analysis. *Nat. Methods*, **9**, 676–682.
16. Restle,A., Farber,M., Baumann,C., Bohringer,M., Scheidtmann,K., Muller-Tidow,C. and Wiesmuller,L. (2008) Dissecting the role of p53 phosphorylation in homologous recombination provides new clues for gain-of-function mutants. *Nucleic Acids Res.*, **36**, 5362–5375.
17. Roemer,K. and Mueller-Lantzsch,N. (1996) p53 transactivation domain mutant Q22, S23 is impaired for repression of promoters and mediation of apoptosis. *Oncogene*, **12**, 2069–2079.
18. Kim,N. and Jinks-Robertson,S. (2017) The Top1 paradox: Friend and foe of the eukaryotic genome. *DNA Repair (Amst.)*, **56**, 33–41.
19. Gobert,C., Skladanowski,A. and Larsen,A.K. (1999) The interaction between p53 and DNA topoisomerase I is regulated differently in cells with wild-type and mutant p53. *Proc National Acad Sci*, **96**, 10355–10360.
20. Sullivan,K.D., Galbraith,M.D., Andrysik,Z. and Espinosa,J.M. (2017) Mechanisms of transcriptional regulation by p53. *Cell Death Differ.*, **25**, 133–143.
21. Maréchal,A. and Zou,L. (2015) RPA-coated single-stranded DNA as a platform for post-translational modifications in the DNA damage response. *Cell Res.*, **25**, 9–23.
22. Smith,L.A., Makarova,A.V., Samson,L., Thiesen,K.E., Dhar,A. and Bessho,T. (2012) Bypass of a psoralen DNA interstrand Cross-Link by DNA polymerases β, ι, and κ in vitro. *Biochemistry-us*, **51**, 8931–8938.
23. Offer,H., Milyavsky,M., Erez,N., Matas,D., Zurer,I., Harris,C.C. and Rotter,V. (2001) Structural and functional involvement of p53 in BER in vitro and in vivo. *Oncogene*, **20**, 581–589.
24. Mansilla,S., Vega,M. de la, Calzetta,N., Siri,S. and Gottifredi,V. (2020) CDK-independent and PCNA-dependent functions of p21 in DNA replication. *Genes-basel*, **11**, 593.
25. Gottifredi,V. and Wiesmüller,L. (2018) The tip of an iceberg: replication-associated functions of the tumor suppressor p53. *Cancers*, **10**, 250.
26. Yeo,C., Alexander,I., Lin,Z., Lim,S., Aning,O., Kumar,R., Sangthongpitag,K., Pendharkar,V., Ho,V.H. and Cheok,C. (2016) p53 maintains genomic stability by preventing interference between transcription and replication. *Cell Rep.*, **15**, 132–146.
27. Gagou,M.E., Zuazua-Villar,P. and Meuth,M. (2010) Enhanced H2AX phosphorylation, DNA replication fork arrest, and cell death in the absence of Chk1. *Mol. Biol. Cell*, **21**, 739–752.
28. Saleh-Gohari,N., Bryant,H.E., Schultz,N., Parker,K.M., Cassel,T.N. and Helleday,T. (2005) Spontaneous homologous recombination is induced by collapsed replication forks that are caused by endogenous DNA single-strand breaks. *Mol. Cell. Biol.*, **25**, 7158–7169.
29. Tomasz,M. (1995) Mitomycin C: small, fast and deadly (but very selective). *Chem. Biol.*, **2**, 575–579.
30. Amunugama,R., Willcox,S., Wu,A.R., Abdullah,U.B., El-Sagheer,A.H., Brown,T., McHugh,P.J., Griffith,J.D. and Walter,J.C. (2018) Replication fork reversal during DNA interstrand crosslink repair requires CMG unloading. *Cell Rep.*, **23**, 3419–3428.
31. Matsumoto,Y., Kim,K. and Bogenhagen,D. (1994) Proliferating cell nuclear antigen-dependent abasic site repair in Xenopus laevis oocytes: an alternative pathway of base excision DNA repair. *Mol. Cell. Biol.*, **14**, 6187–6197.
32. Fan,J., Otterlei,M., Wong,H., Tomkinson,A.E. and Wilson,D.M. (2004) XRCC1 co-localizes and physically interacts with PCNA. *Nucleic Acids Res.*, **32**, 2193–2201.
33. Petta,T.B., Nakajima,S., Zlatanou,A., Despras,E., Couve-Privat,S., Ishchenko,A., Sarasin,A., Yasui,A. and Kannouche,P. (2008) Human DNA polymerase iota protects cells against oxidative stress. *EMBO J.*, **27**, 2883–2895.
34. Kern,S., Kinzler,K., Bruskin,A., Jarosz,D., Friedman,P., Prives,C. and Vogelstein,B. (1991) Identification of p53 as a sequence-specific DNA-binding protein. *Science*, **252**, 1708–1711.
35. Zambetti,G., Bargonetti,J., Walker,K., Prives,C. and Levine,A. (1992) Wild-type p53 mediates positive regulation of gene expression through a specific DNA sequence element. *Gene Dev*, **6**, 1143–1152.
36. Dudenhöffer,C., Rohaly,G., Will,K., Deppert,W. and Wiesmüller,L. (1998) Specific mismatch recognition in heteroduplex intermediates by p53 suggests a role in fidelity control of homologous recombination. *Mol. Cell. Biol.*, **18**, 5332–5342.
37. Lee,S., Cavallo,L. and Griffith,J. (1997) Human p53 binds holliday junctions strongly and facilitates their cleavage. *J. Biol. Chem.*, **272**, 7532–7539.
38. Ory,K., Legros,Y., Auguin,C. and Soussi,T. (1994) Analysis of the most representative tumour-derived p53 mutants reveals that changes in protein conformation are not correlated with loss of transactivation or inhibition of cell proliferation. *EMBO J.*, **13**, 3496–3504.
39. Dudenhöffer,C., Kurth,M., Janus,F., Deppert,W. and Wiesmüller,L. (1999) Dissociation of the recombination control and the sequence-specific transactivation function of P53. *Oncogene*, **18**, 1202964.
40. Espinosa,J.M. and Emerson,B.M. (2001) Transcriptional regulation by p53 through intrinsic DNA/Chromatin binding and site-directed cofactor recruitment. *Mol. Cell*, **8**, 57–69.
41. Livneh,Z. (2006) Keeping mammalian mutation load in check: regulation of the activity of error-prone DNA polymerases by p53 and p21. *Cell Cycle*, **5**, 1918–1922.
42. Janus,F., Albrechtsen,N., Knippschild,U., Wiesmüller,L., Grosse,F. and Deppert,W. (1999) Different regulation of the p53 core domain activities 3′-to-5′ exonuclease and Sequence-Specific DNA binding. *Mol. Cell. Biol.*, **19**, 2155–2168.
43. Lin,J.-R., Zeman,M.K., Chen,J.-Y., Yee,M.-C. and Cimprich,K.A. (2011) SHPRH and HLTF act in a damage-specific manner to coordinate different forms of postreplication repair and prevent mutagenesis. *Mol. Cell*, **42**, 237–249.
44. Manzo,S.G., Hartono,S.R., Sanz,L.A., Marinello,J., Biasi,S.D., Cossarizza,A., Capranico,G. and Chedin,F. (2018) DNA Topoisomerase I differentially modulates R-loops across the human genome. *Genome Biol.*, **19**, 100.
45. Ji,P., Agrawal,S., Diederichs,S., Bäumer,N., Becker,A., Cauvet,T., Kowski,S., Beger,C., Welte,K., Berdel,W.E. *et al.* (2004) Cyclin A1, the alternative A-type cyclin, contributes to G1/S cell cycle progression in somatic cells. *Oncogene*, **24**, 2739–2744.
46. Dutta,A., Ruppert,M.J., Aster,J.C. and Winchester,E. (1993) Inhibition of DNA replication factor RPA by p53. *Nature*, **365**, 79–82.
47. Kaustov,L., Yi,G.-S., Ayed,A., Bochkareva,E., Bochkarev,A. and Arrowsmith,C.H. (2006) p53 transcriptional activation domain: a molecular chameleon? *Cell Cycle*, **5**, 489–494.

48. Miller,S., Moses,K., Jayaraman,L. and Prives,C. (1997) Complex formation between p53 and replication protein A inhibits the sequence-specific DNA binding of p53 and is regulated by single-stranded DNA. *Mol. Cell. Biol.*, **17**, 2194–2201.
49. Zhou,J., Ahn,J., Wilson,S. and Prives,C. (2001) A role for p53 in base excision repair. *EMBO J.*, **20**, 914–923.
50. Haupt,Y., Maya,R., Kazaz,A. and Oren,M. (1997) Mdm2 promotes the rapid degradation of p53. *Nature*, **387**, 296–299.
51. Oliner,J.D., Pietenpol,J.A., Thiagalingam,S., Gyuris,J., Kinzler,K.W. and Vogelstein,B. (1993) Oncoprotein MDM2 conceals the activation domain of tumour suppressor p53. *Nature*, **362**, 857–860.
52. Levine,A.J. and Oren,M. (2009) The first 30 years of p53: growing ever more complex. *Nat. Rev. Cancer*, **9**, 749–758.
53. Klusmann,I., Wohlberedt,K., Magerhans,A., Teloni,F., Korbel,J.O., Altmeyer,M. and Dobbelstein,M. (2018) Chromatin modifiers Mdm2 and RNF2 prevent RNA:DNA hybrids that impair DNA replication. *Proc. Natl. Acad. Sci. U.S.A.*, **115**, E11311–E11320.
54. Bertolin,A.P., Mansilla,S.F. and Gottifredi,V. (2015) The identification of translesion DNA synthesis regulators: Inhibitors in the spotlight. *DNA Repair (Amst.)*, **32**, 158–164.
55. Ashcroft,M., Kubbutat,M.H. and Vousden,K.H. (1999) Regulation of p53 function and stability by phosphorylation. *Mol. Cell. Biol.*, **19**, 1751–1758.
56. Shieh,S.-Y., Ikeda,M., Taya,Y. and Prives,C. (1997) DNA damage-induced phosphorylation of p53 alleviates inhibition by MDM2. *Cell*, **91**, 325–334.
57. Sengupta,S. and Harris,C.C. (2005) p53: traffic cop at the crossroads of DNA repair and recombination. *Nat. Rev. Mol. Cell Biol.*, **6**, 44–55.
58. Banks,D., Wu,M., Higa,L., Gavrilova,N., Quan,J., Ye,T., Kobayashi,R., Sun,H. and Zhang,H. (2006) L2DTL/CDT2 and PCNA interact with p53 and regulate p53 polyubiquitination and protein stability through MDM2 and CUL4A/DDB1 complexes. *Cell Cycle*, **5**, 1719–1729.
59. Stallons,J.L. and McGregor,G.W. (2010) Translesion synthesis polymerases in the prevention and promotion of carcinogenesis. *J. Nucleic Acids*, **2010**, 643857.
60. Vujanovic,M., Krietsch,J., Raso,M., Terraneo,N., Zellweger,R., Schmid,J.A., Taglialatela,A., Huang,J.-W., Holland,C.L., Zwicky,K. *et al.* (2017) Replication fork slowing and reversal upon DNA damage require PCNA Polyubiquitination and ZRANB3 DNA translocase activity. *Mol. Cell*, **67**, 882–890.
61. Bai,G., Kermi,C., Stoy,H., Schiltz,C.J., Bacal,J., Zaino,A.M., Hadden,K.M., Eichman,B.F., Lopes,M. and Cimprich,K.A. (2020) HLTF promotes fork reversal, limiting replication stress resistance and preventing multiple mechanisms of unrestrained DNA synthesis. *Mol. Cell*, **78**, 1237–1251.